RESEARCH ARTICLE | JULY 11 2023

Rotational circular dichroism of diamagnetic and paramagnetic molecules. A computational study

Jiří Zdráhala ; Petr Bouř

J. Chem. Phys. 159, 024115 (2023)
https://doi.org/10.1063/5.0156273

The Journal of Chemical Physics ARTICLE pubs.aip.org/aip/jcp

Rotational circular dichroism of diamagnetic and paramagnetic molecules. A computational study

Cite as: J. Chem. Phys. 159, 024115 (2023); doi: 10.1063/5.0156273
Submitted: 28 April 2023 • Accepted: 16 June 2023 •
Published Online: 11 July 2023

Jiří Zdráhala[1,2] and Petr Bouř[1,2,a)]

AFFILIATIONS

[1] Institute of Organic Chemistry and Biochemistry, Academy of Sciences, Flemingovo náměstí 2, 16610 Prague, Czech Republic
[2] Department of Analytical Chemistry, University of Chemistry and Technology, Technická 5, 16628 Prague, Czech Republic

[a)] **Author to whom correspondence should be addressed:** bour@uochb.cas.cz

ABSTRACT

Rotational circular dichroism (RCD) has not been observed yet, but it is expected to deliver information about chiral molecules useful in many branches of chemistry. In the past, rather weak RCD intensities were predicted for model diamagnetic molecules and a limited number of rotational transitions. Here, we review quantum-mechanical foundations and simulate entire spectral profiles, including larger molecules, open-shell molecular radicals, and high-momentum rotational bands. Contribution of the electric quadrupolar moment was considered, but it turned out that it does not contribute to field-free RCD. Two conformers of a model dipeptide provided clearly distinct spectra. The dissymmetry Kuhn parameter g_K predicted for the diamagnetic molecules even for high-J transitions rarely exceeded 10^{-5}, and the simulated RCD spectra were often biased to one sign. In the radicals, the coupling of the rotational angular momentum with the spin for some transitions raised g_K to about 10^{-2}, and the RCD pattern was more conservative. In the resultant spectra, many transitions had negligible intensities due to small populations of the involved states, and a convolution with a spectral function made the typical RCD/absorption ratios about 100-times smaller ($g_K \sim 10^{-4}$). This is still comparable with values typical for electronic or vibrational circular dichroism, and paramagnetic RCD is thus likely to be measurable relatively easily.

I. INTRODUCTION

Circular dichroism (CD), differential absorption of the left and right circularly polarized light, is indispensable for studies of optically active molecules. Compared to plain absorption of unpolarized light, CD spectra are more sensitive to molecular structure or conformation. Molecular enantiomers provide CD bands of the same frequency and intensity, but of opposite signs. In the ultraviolet and visible region, electronic CD (ECD) spectroscopy became a standard method to study inorganic and organic molecules, including proteins, sugars, nucleic acids, and pharmaceuticals.[1,2] Similarly successful as ECD was vibrational CD (VCD) using infrared light.[3,4] In addition, VCD bands were more numerous, better resolved, and easier to interpret than for ECD.[5,6]

Rotational CD (RCD), the difference in absorption of left and right circular polarized light for rotational transitions, has not yet been reported. These transitions are typically observed with microwave radiation of frequencies within about 6–20 GHz (wavelength 1.5–5 cm). Although the microwave gas spectra provide impressive resolution,[7] the technology, in general, struggles with accurate intensity measurement.[8,9]

Yet, optically active systems are increasingly studied by rotational spectroscopy, and the need for methods sensitive to chirality in the gas phase is apparent.[10,11] Recent instrumental developments led to several new experiments meant to distinguish enantiomers and measure the enantiomeric excess. These include microwave three-wave mixing,[12] photoelectron circular dichroism using circularly polarized laser light or synchrotron sources,[13,14] and Coulomb explosion with coincidence imaging.[15] In addition, chiral-tagging becomes popular, where the chirality is recognized on the basis of non-covalently bound diastereoisomer formation.[10,16]

Analogous chirality detection by RCD is complicated by the small ratio of the chiral signal to the total absorption for a given transition, known as the Kuhn anisotropy or dissymmetry factor g_K. In the past, Salzman and co-workers predicted that for model diamagnetic molecules, the factor only rarely exceeds 10^{-5}, and for most transitions, it stays at $\sim 10^{-7}$ and lower.[17–25] They also formulated a semiclassical theory of RCD and showed that the permanent electric dipole moment and the gyromagnetic tensor ("g-tensor") are the principle molecular properties determining the intensities. Polavarapu found an interesting relation between vibrational and rotational CD.[26] In addition, rotational Raman optical activity (ROA) in chiral molecules has been considered,[26,27] but not observed experimentally. Measurements of optical activity in the gas phase without high rotational resolution are relatively frequent. For example, VCD and ROA of methyloxirane,[28,29] magnetic resonance ROA of paramagnetic[30] and diamagnetic[31] gases, and ECD of many molecules[32] were reported.

In the present work, to provide a general guidance to future RCD explorations, we review in detail the theory based on the rigid rotor approximation, perform simulations at realistic temperature for a broader class of molecules, and include high vibrational quantum numbers for high-energy transitions. In the theory, we incorporate the electric quadrupole contribution. It vanishes for the cases treated in the present study, but may be important for oriented samples, e.g., under the presence of electric or magnetic fields. With dedicated software, we also investigate model conformers and paramagnetic molecules. In the paramagnetic case, the electronic spin couples with the rotational motion and the g_K factor can dramatically increase, which can be approximately related to the ratio of the nuclear and Bohr magnetons ($\mu_B/\mu_N \sim 1800$). In addition, electronic and typical molecular gyromagnetic ratios are in relation ($g_e/g \sim 10$) favorable for the RCD of radicals. This indicates that paramagnetic molecules, such as the radicals, might be the most suitable systems for RCD experiments in the future.

II. THEORY

A. RCD of diamagnetic molecules

We assume a rigid rotor Hamiltonian,[33,34]

$$H = AJ_a^2 + BJ_b^2 + CJ_c^2, \tag{1}$$

where A, B, and C are the rotational constants and J_a, J_b, and J_c are the components of the angular momentum $\mathbf{J}$ in the molecule fixed axes a, b, and c. From the Schrödinger equation, we get the wave function expanded in the symmetric rotor basis $|J,K,M\rangle$ as[34]

$$\Psi_i(J,M) = |i\rangle = \sum_{K=-J}^{J} c_{iK}|J,K,M\rangle, \tag{2}$$

where c_{iK} are the expansion coefficients, K and M are projections of $\mathbf{J}$ on the molecular and space axis, respectively, and J is the angular momentum quantum number.

Let us suppose that the light propagates along the space axis Z. Following Ref. 35 [Eq. (3.4.39) therein] and Ref. 17, we introduce the dipole (D_{ij}) and rotational (R_{ij}) strengths for a rotational transition $i \to j$ as

$$D_{ij} = \frac{1}{2J+1}\sum_{M,M;}\left(\mu_{X,ij}\mu_{X,ji} + \mu_{Y,ij}\mu_{Y,ji}\right) = \frac{2}{2J+1}\sum_{M,M;}\mu_{X,ij}\mu_{X,ji}, \tag{3}$$

$$R_{ij} = R_{m,ij} + R_{\Theta,ij}, \tag{4}$$

where

$$R_{m,ij} = \frac{1}{2J+1}\mathrm{Im}\sum_{M,M;}\left(\mu_{X,ij}m_{X,ji} + \mu_{Y,ij}m_{Y,ji}\right) = \frac{2}{2J+1}\mathrm{Im}\sum_{M,M;}\mu_{X,ij}m_{X,ji},$$

$$R_{\Theta,ij} = \frac{1}{2J+1}\frac{\omega_{ij}}{3}\mathrm{Re}\sum_{M,M;}\left(\mu_{Y,ij}\Theta_{XZ,ji} - \mu_{X,ij}\Theta_{YZ,ji}\right) = \frac{1}{2J+1}\frac{\omega_{ij}}{3}\mathrm{Re}\sum_{M,M'}\sum_{A,B}\varepsilon_{ABZ}\mu_{B,ij}\Theta_{AZ,ji}.$$

μ, m, and Θ is the electric dipole, magnetic dipole, and electric quadrupole operator, respectively; $\omega_{ji} = \omega_j - \omega_i$ is the difference of angular frequencies of the two states; ε_{ABZ} are elements of the antisymmetric tensor; and M and M' change from $-J$ to J. The transition integrals are abbreviated as $\mu_{X,ij} = \langle i|\mu_X|j\rangle$. For D_{ij} and $R_{m,ij}$, we used the fact that the choice of the X and Y axes is arbitrary and the X and Y components must contribute equally. Using (2), the matrix elements of the operators ($o = \mu_F$, m_F, Θ_{FG}) in (3) and (4) can be written as

$$o_{ij} = \sum_{K,K'} c_{iK}^* c_{jK'}\langle J,K,M|o|J',K',M'\rangle. \tag{5}$$

Next, we need to transform molecular properties from the molecule fixed coordinates ($\alpha = x$, y, or z, small letters) to the space fixed ones ($F = X$, Y, or Z, capitals). For μ, we can write

$$\mu_F = \sum_{\alpha}\lambda_{F\alpha}\mu_\alpha, \tag{6}$$

where $\lambda_{F\alpha}$ are the Cartesian direction cosines.[34] Using (5), we arrive at the direction cosine integrals in the rigid rotor basis, which can be factorized as

$$\langle JKM|\lambda_{F\alpha}|J'K'M'\rangle = (JJ')(JK\alpha J'K')(JMFJ'M'). \tag{7}$$

The identity

$$\sum_{M,M'}(JMXJ'M')(J'M'XJM) = 2\sum_{M}(JMXJ'M+1)\times(J'M+1XJM), \tag{8}$$

and Eqs. (2), (3), and (6) allow us to write the dipole strength in a more explicit form,

$$D_{ij} = \frac{4}{2J+1}\mu_{ij}\mu_{ji}\sum_{M}(JMXJ'M+1)(J'M+1XJM), \tag{9}$$

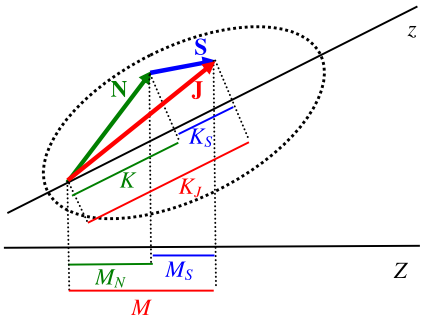

FIG. 1. The rotational **N**, spin **S**, and total **J** angular momenta in a paramagnetic molecule and their projections onto molecular *z* and space *Z* fixed axes.

where the reduced matrix elements $\mu_{ij} = (JJ')\sum_{\alpha}\sum_{K}\sum_{K'} c^{*}_{iK}c_{jK'}\mu_{\alpha}(JK\alpha J'K')$.

Similarly, the magnetic dipole moment in the molecule fixed axes is[17]

$$m_{\alpha} = \mu_N \sum_{\beta} g_{\alpha\beta} J_{\beta}, \tag{10}$$

where μ_N is the nuclear magneton and $g_{\alpha\beta}$ are components of the rotational *g*-tensor. However, the direction cosine elements do not commute with the *J* operators, and we cannot use a transformation analogous to Eq. (6) directly. Instead, to ensure hermicity of the magnetic moment in the space fixed axes, we introduce the anti-commutator $\{\lambda_{F\alpha}, J_{\beta}\} = \lambda_{F\alpha}J_{\beta} + J_{\beta}\lambda_{F\alpha}$ so that[36]

$$m_F = \frac{1}{2}\mu_N \sum_{\beta}\sum_{\alpha} g_{\alpha\beta}\{\lambda_{F\alpha}, J_{\beta}\}. \tag{11}$$

Using Ref. 37, $\{\lambda_{F\alpha}, J_{\beta}\} = 2\lambda_{F\alpha}J_{\beta} + i\hbar\sum_{\gamma}\varepsilon_{\alpha\beta\gamma}\lambda_{F\gamma}$, and defining a mixed Cartesian-spherical form of the *g*-tensor, $g_{\alpha\pm} = \frac{1}{2}(g_{\alpha x} \pm i g_{\alpha y})$, we get

$$m_F = \mu_N \sum_{\alpha}\left[\lambda_{F\alpha}\left(g_{\alpha+}J^{(m)}_{-} + g_{\alpha-}J^{(m)}_{+} + g_{\alpha z}J_z\right) + \frac{i\hbar}{2}\sum_{\beta} g_{\alpha\beta}\sum_{\gamma}\varepsilon_{\alpha\beta\gamma}\lambda_{F\gamma}\right], \tag{12}$$

where $J^{(m)}_{\pm} = J_x \pm iJ_y$ and $\varepsilon_{\alpha\beta\gamma}$ is the antisymmetric tensor. Finally, for the rotational strength $R_{m,ij}$, from (4), (5), and (12), we get

$$R_{m,ij} = \frac{4}{2J+1} Im\mu_{ij}m_{ji}\sum_{M}(JMXJ'M+1)(J'M+1XJM), \tag{13}$$

where the reduced matrix elements

$$m_{ji} = \mu_N(JJ')\sum_{K,K'} c^{*}_{jK'}c_{iK}\sum_{\alpha}\left\{g_{\alpha+}f_{JK+}(J'K'\alpha JK+1)\right.$$
$$\left. + g_{\alpha-}f_{JK-}(J'K'\alpha JK-1) + \left(g_{\alpha z} + \frac{i\hbar}{2}\sum_{\beta}\sum_{\gamma}\varepsilon_{\gamma\alpha\beta}g_{\beta\gamma}\right)(J'K'\alpha JK)\right\},$$

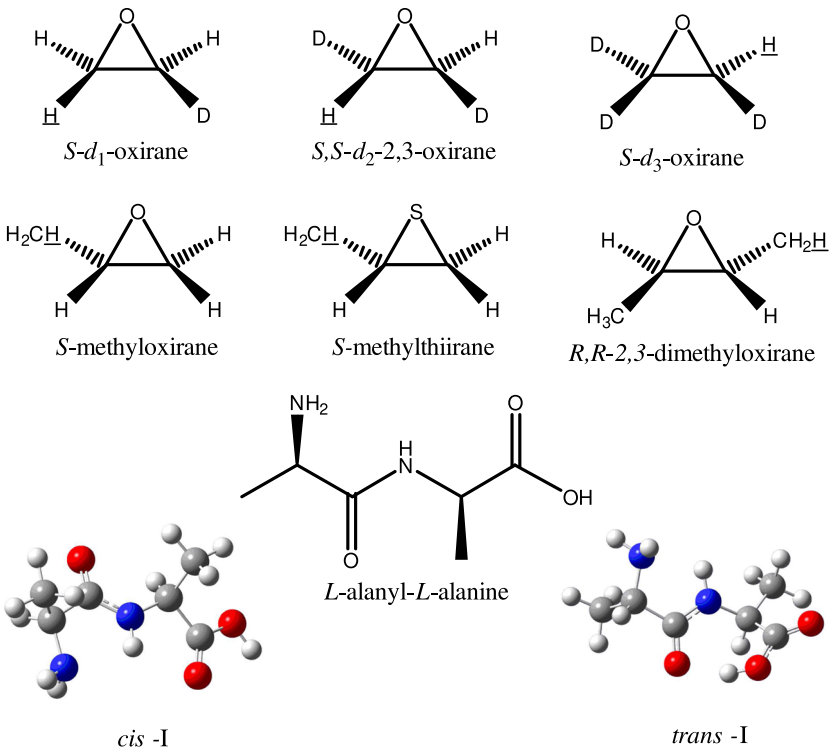

FIG. 2. Investigated systems: six "small" molecules and two *l*-alanyl-*l*-alanine ("dialanine") conformers (*cis*-I, *trans*-I according to Ref. 41). From the small molecules, radicals were formed by removing the underlined hydrogen atoms.

where $f_{JK\pm} = \sqrt{J(J+1) - K(K\pm 1)}$ are eigenvalues of the ladder operators and $J_{\pm}^{(m)}|J,K,M\rangle = f_{JK\pm}|J,K\mp 1,M\rangle$.

The g-tensor is a sum of the nuclear and electronic parts,[38] $g = g^n + g^e$, with

$$g^n_{\alpha\beta} = m_p \sum_i Z_i \left(R_i^2 \delta_{\alpha\beta} - R_{i\alpha} R_{i\beta}\right)/I_\alpha, \tag{14}$$

$$g^e_{\alpha\beta} = -4 m_p \chi^p_{\alpha\beta}/I_\alpha, \tag{15}$$

where m_p is the mass of the proton, Z_i is the atomic number, R_i is the position of nucleus i, I is the moment of inertia, and $\chi^p_{\alpha\beta}$ is the paramagnetic susceptibility.

Quadrupole components in the space fixed frame are

$$\Theta_{FG} = \sum_\alpha \sum_\beta \lambda_{F\alpha} \lambda_{G\beta} \Theta_{\alpha\beta}, \tag{16}$$

TABLE I. Examples of dipole (D/debye^2) and rotational (R/10^{-8} debye^2) strengths and the Kuhn parameter ($g_K = 4R/D$) calculated for some high-g_K transitions in diamagnetic molecules.

$J_{Ka,Kc}$ (excited)	$J_{Ka,Kc}$ (ground)	ν (GHz)	D	R	$g_K \times 10^6$
		S-d_1-oxirane			
$52_{50,2}$	$51_{49,3}$	2487.582	1.078	−150	−5.57
$59_{51,8}$	$59_{50,10}$	678.686	0.265	−36	−5.47
$31_{31,1}$	$30_{30,1}$	1496.645	1.140	−99	−3.44
		S,*S*-d_2-2,3-oxirane			
$58_{58,0}$	$57_{57,1}$	2654.421	1.186	−322	−10.87
$37_{37,1}$	$36_{36,1}$	1690.796	1.183	−204	−6.90
$39_{11,28}$	$39_{10,29}$	420.5781	0.412	−61	−5.94
		S-d_3-oxirane			
$60_{60,1}$	$59_{59,1}$	2586.641	1.178	149	5.05
$77_{1,77}$	$76_{0,76}$	1862.442	1.175	−113	−3.84
$37_{26,12}$	$37_{25,13}$	329.7232	0.480	29	2.43
		S-methyloxirane			
$77_{77,1}$	$76_{76,1}$	2763.952	2.412	388	6.45
$23_{6,18}$	$23_{5,18}$	119.4093	0.062	8	5.38
$53_{53,1}$	$52_{52,0}$	1898.813	2.411	267	4.42
		S-methylthiirane			
$97_{97,1}$	$96_{96,1}$	2252.669	0.748	185	9.90
$61_{61,1}$	$60_{60,1}$	1413.944	0.748	116	6.20
$39_{39,1}$	$38_{38,1}$	901.3899	0.748	74	3.94
		R,*R*-2,3-dimethyloxirane			
$94_{94,1}$	$93_{93,0}$	2290.972	2.9202	424	5.80
$78_{78,0}$	$77_{77,1}$	1899.49	2.9202	351	4.81
$37_{37,1}$	$36_{36,1}$	896.3172	2.9197	165	2.26

where the α and β indices refer to the molecule fixed system. The quadrupolar part of the rotational strength (4) is then

$$R_{\Theta,ij} = \frac{1}{2J+1} \frac{\omega_{ji}}{3} \mu_{ij} \sum_{J''} \Theta_{J'',ij} \sum_{A,B} \varepsilon_{ZAB} \times \sum_{M,M'} (JMBJ'M')(J'M'AJ''M)(J''MZJM), \tag{17}$$

where the reduced matrix element

$$\Theta_{J'',ij} = \sum_{K,K'} C^*_{iK} C_{jK'} (J'J'')(J''J) \times \sum_{K''} \sum_\alpha \sum_\beta \Theta_{\alpha\beta} (J'K'\alpha J''K'')(J''K''\beta JK).$$

Computationally, we found that for any tried transition, $R_{\Theta,ij} = 0$. However, we did not discover a simple analytical proof of this. For example, neither $\Theta_{J'',ij}$ nor the sum after it in (17) is, in general, zero.

B. RCD of a paramagnetic molecule

For the case of non-zero spin **S**, the total angular momentum is **J** = **N** + **S**, where **N** is the mechanical angular momentum. We consider the Hamiltonian as a sum of the rotational H_0 and spin-rotational H_{SR} parts,[39]

$$H = (AN_a^2 + BN_b^2 + CN_c^2) + \frac{1}{2} \sum_{\alpha,\beta} e_{\alpha\beta} (N_\alpha S_\beta + S_\beta N_\alpha) = H_0 + H_{SR}, \tag{18}$$

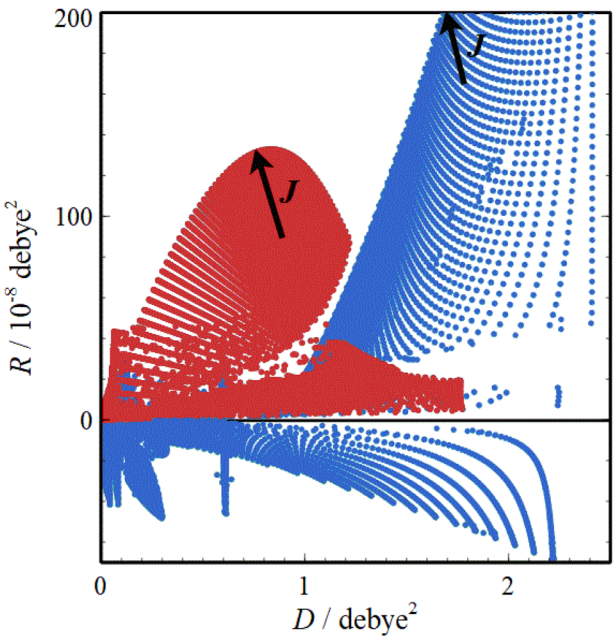

FIG. 3. *S*-methyloxirane and dipole (D) and rotational (R) strengths calculated for vibrational transitions up to $J = 100$; red points are for $\Delta J = 0$ and blue ones for $\Delta J = 1$. The arrows indicate growing J.

where $e_{\alpha\beta}$ is the spin-rotation interaction tensor. Similarly, as in the diamagnetic case, the wave function is

$$\Psi_i = \sum_{N=|J-S|}^{|J+S|} \sum_{K=-N}^{N} C_{iKN} |NKSJM\rangle, \tag{19}$$

where $|NKSJM\rangle$ are uncoupled basis functions,[39] K is the projection of **N** onto the molecule fixed z axis, and M is the projection of **J** onto the space fixed Z axis (Fig. 1). The basis functions themselves can be expressed in a basis from rigid rotor and spin wave functions as

$$|NKSJM\rangle = \sum_{M_N M_S} \langle NM_N SM_S|JK\rangle |NKM_N\rangle |SM_S\rangle, \tag{20}$$

where $\langle NM_N SM_S|JM\rangle$ are the Clebsch–Gordan coefficients.[40] Then, the evaluation of the Hamiltonian matrix elements, such as $\langle N'K'SJM|H_{SR}|NKSJM\rangle$, is straightforward when we realize the relation between the molecule-fixed S_α and space-fixed S_F spin, $S_\alpha = \sum_F \lambda_{F\alpha} S_F$.

The transition electric dipole moment needed in (3) can be obtained directly using relations (6), (7), (19), and (20). The magnetic moment is a sum of the rotational and spin parts,

$$\mathbf{m} = \mathbf{m}_R + \mathbf{m}_S = \mu_N \mathbf{g} \cdot \mathbf{N} + \mu_B g_e \mathbf{S}, \tag{21}$$

where $g_e = 2.002\,319$, **g** is the rotational g-tensor, and μ_N and μ_B is, respectively, the nuclear and Bohr magneton. For the rotational part, we can follow Eqs. (10)–(12), replacing J by N, while for the spin one, we get

$$\begin{aligned} m_{SF,ji} &= \langle j|m_{SF}|i\rangle \\ &= \frac{\mu_B g_e}{2p} (\delta_{M'M+1} \pm \delta_{M'M-1}) \sum_{KN} C^*_{jKN} C_{iKN} \\ &\quad \times \sum_{M_N} \langle J'M'|NM_N S, M' - M_N\rangle \\ &\quad \times \langle NM_N S, M - M_N|JM\rangle, \end{aligned} \tag{22}$$

where the plus sign and $p = 1$ holds for $F = X$ and minus and $p = i$ for $F = Y$.

III. COMPUTATIONS

Model molecules are summarized in Fig. 2. The oxirane derivatives are convenient small chiral rigid molecules, and some were already used for RCD predictions by Salzman.[17,18] Methyloxirane is the first chiral molecule detected in the interstellar space,[42] which sparked speculations in astrobiology,[43] and its circular dichroism in the microwave region has been predicted for some torsion-rotation transitions.[44] Dialanine was added to investigate spectral differences in molecular conformers; it also serves as a biologically relevant model in rotational spectroscopy.[41] In addition, six radicals were

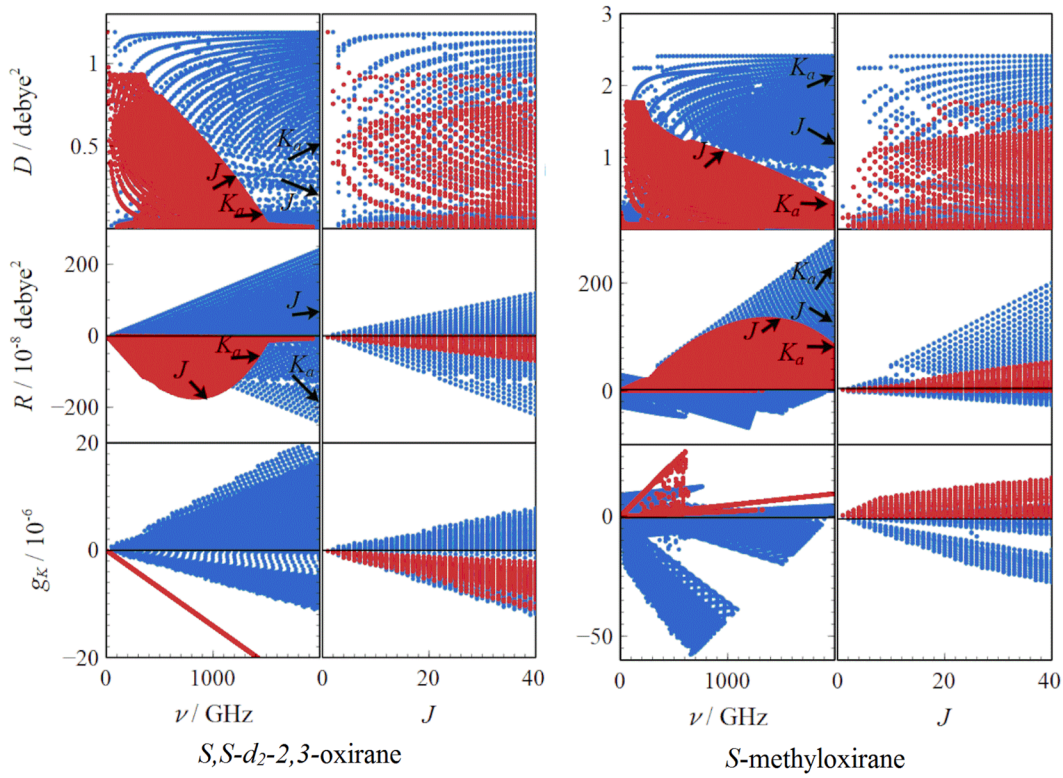

FIG. 4. *S,S*-d_2-2,3-oxirane and *S*-methyloxirane: dipole (D) and rotational (R) strengths and the g_K ratio dependent on the transition frequency ν and J; red for $\Delta J = 0$ and blue for $\Delta J = 1$.

made by removing hydrogen atoms from oxiranes and thiirane. Although the theory presented above is universal, the RCD experiment might be quite difficult for molecules significantly larger than those in the chosen set.

The geometries were optimized by energy minimization using the Gaussian[45] software and the B3LYP/6-311++G** level of theory. The *g*-and spin-rotation interaction tensors and permanent electric dipole moments were calculated at the CAM-B3LYP/aug-cc-pVTZ level. The gauge independent atomic orbitals (GIAOs) were used for the magnetic properties to achieve gauge invariance. The CAM-B3LYP functional and larger basis set was recommended for molecular magnetic properties.[46] For the three-member ring molecules, the electric dipole moments were taken from Ref. 25. When available, experimental rotational constants were used; otherwise, values calculated for the optimized geometry were taken. The computational parameters are listed in the supplementary material, Tables SI and SII. For the *S*-methyloxirane radical, the dipole moment and *g* and *e*-tensors were also calculated using smaller (aug-cc-pVDZ) and two larger (aug-cc-pVQZ and aug-cc-pVQZ) bases sets (Table SIII), which in final effect led to rather negligible changes in the spectra

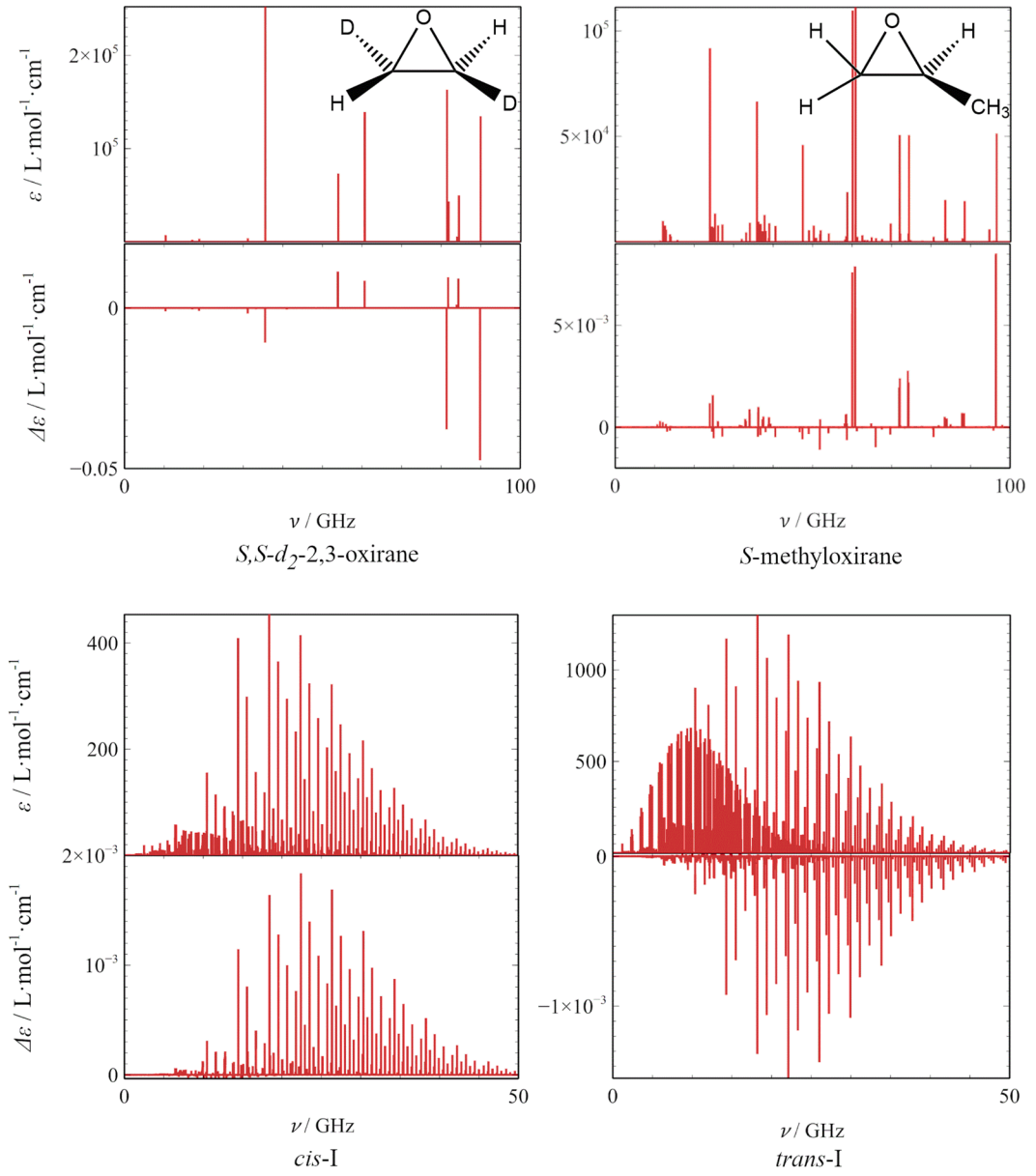

FIG. 5. Simulated absorption and RCD spectra of *S*,*S*-d_2-2,3-oxirane, *S*-methyloxirane, and *cis*-I and *trans*-I dialanine conformers at 2 K.

(Fig. S1). This is consistent with previous basis set studies. For example, already, relatively small basis sets reasonably well reproduced the g-tensor.[47]

The absorption $\varepsilon(\nu)$ and RCD $\Delta\varepsilon(\nu)$ spectral intensities (in l mol^{-1} cm^{-1}) were obtained as

$$\varepsilon(\nu) = D_{ij}\, f(\nu), \tag{23}$$

$$\Delta\varepsilon(\nu) = 4R_{ij}\, f(\nu), \tag{24}$$

where $f(\nu) = 108.862 \times \nu_{ij} D_{ij} [e^{-h\nu_i/(KT)} - e^{-h\nu_j/(KT)}] Q^{-1} S(\nu)$, $\nu_{ij} = \nu_j - \nu_i$ is the difference of state frequencies for a transition $i \to j$, h is the Planck constant, k is the Boltzmann constant, T is the temperature (by default T = 2 K), the strengths R and D are in debye^2, and Q is the rotational partition function,[48]

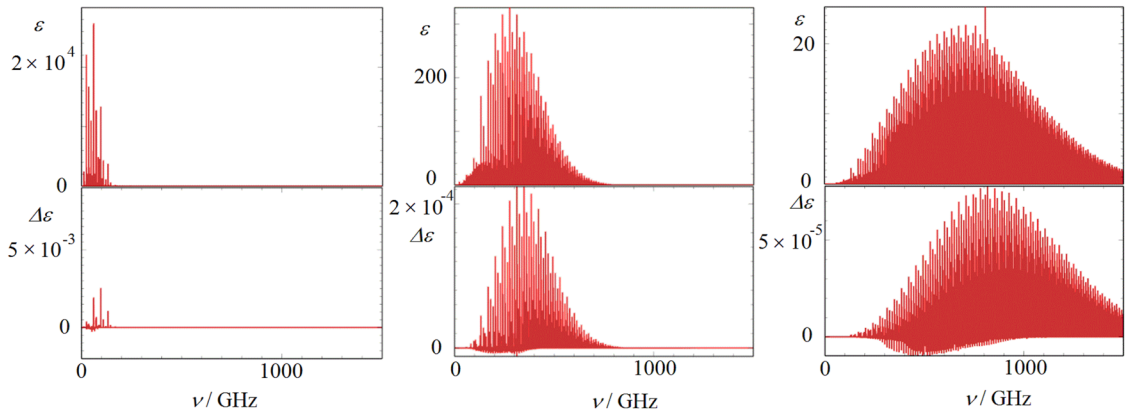

FIG. 6. Simulated absorption and RCD spectra of *S*-methyloxirane at 2, 50, and 300 K.

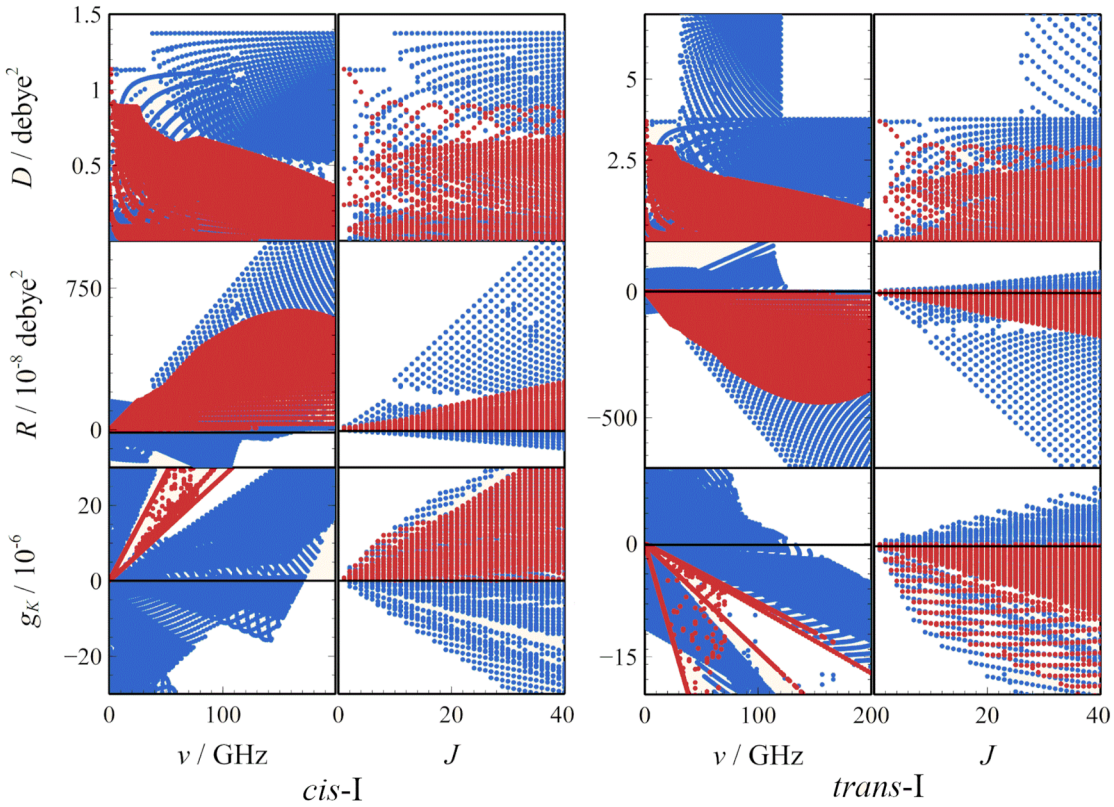

FIG. 7. *Cis*-l and *trans*-l dialanine conformers, dipole (D) and rotational (R) strengths, and the g_K ratio dependent on the transition frequency ν and J; red for $\Delta J = 0$ and blue for $\Delta J = 1$.

$$Q = \frac{1}{\sigma}\sqrt{\frac{\pi k^3 T^3}{h^3 ABC}}M, \tag{25}$$

where σ is the symmetry number and $M = 2S + 1$ is the multiplicity. A Lorentzian spectral function was used, $S(\nu) = \frac{1}{\pi}\frac{\Delta}{(\nu-\nu_{ij})^2+\Delta^2}$, with $\Delta = 1$ MHz. For control, absorption intensities were also compared to results obtained from the SPCAT[49] and ASROT[50] programs.

IV. RESULTS AND DISCUSSION

A. RCD of diamagnetic molecules

For low-J transitions, where analytical relations were available, our results agreed with the previously published values.[24] In addition, other numerical simulations qualitatively agree with the literature values; several transitions for S-methyloxirane obtained in this work are compared with the literature values in Table SIV. The g_K factor for S-methyloxirane does not exceed 10^{-5}; for S-d_3-oxirane and S-d_1-oxirane, low-J transitions with $g_K \sim 10^{-4}$ were predicted; these, however, are associated with small dipole strengths and may not be detectable. In methyloxirane, for example, the average dipole strength is $D_{ave} = 0.14$ D^2 with root mean square deviation $D_{rms} = 0.39$, that is, 274% of D_{ave}. For the rotational strength, $|R|_{ave} = 9.2 \times 10^{-8}$ and $|R|_{rms} = 1.06 \times 10^{-8} = 391\%$ of $|R|_{ave}$. These changes, in both the dipole and rotational strengths, cause large variations of the g_K parameter.

The situation is somewhat different for high-J transitions. Some of them, those with high g_K–factors, are listed for the six model molecules in Table I, and more of them can be found in Table SV. The states are labeled using the near symmetry quantum numbers[34] K_a and K_c. The transitions were selected within the 2–3000 GHz range, comprising J up to 100. Occasionally, g_K is high because the dipole strength is small (the $23_{5,18} \rightarrow 23_{6,18}$ transition in S-methyloxirane, Table I). In the majority of cases, however, g_K grows because while the dipole strength is constant, limited by the permanent dipole, the magnetic moment and, thus, the rotational strength grow.

For S-methyloxirane, trends in the dipole and rotational strengths as dependent on J are represented in Fig. 3. The dependencies for the other molecules were similar (Fig. S2, left). The dipole strength is roughly limited by the permanent molecular dipole, which can also be seen from Eq. (9). Here, we sum over $2J + 1$ values of M. The $2J + 1$ factor cancels out with the denominator since the cosine matrix elements are limited by a constant for high J [Eq. (7), Table SVI]. On the other hand, the magnetic moment and rotational strength contain an additional power of J [cf. Eq. (10)] and thus may grow steadily with it. In Fig. 3, we see a relatively simple dependence for $\Delta J = 1$: for high Js, the dipole strength is limited by ~2.4 D^2, while Rs grow outside the displayed range. For the case of $\Delta J = 0$, the relations are more complex.

For an alternate insight, the dependencies of the dipole and rotational strengths and the g_K factor on the transition frequency and J are plotted for S,S-d_2-2,3-oxirane and S-methyloxirane in Fig. 4. Again, we can see the limit of the dipole strength and the growth of R and g_K. Both the $\Delta J = 1$ and $\Delta J = 0$ transitions can exhibit relatively large g_Ks; transition with $\Delta J = 0$ occurs in smaller frequencies, perhaps better achievable by common microwave techniques. For larger or heavier molecules with smaller rotational constants, however, much more transitions will be observable in the millimeter (30–300 GHz) or centimeter (3–30 GHz) wavelength regions.

From these dependencies, we can also see that the intensities of the absorption and RCD lines are not simple functions of the permanent dipole and the g-tensor. The largest Rs and g_Ks exhibit methyloxirane, probably because of the large difference of xz and zx g-tensor components (diagonal g-components do not contribute to RCD). Approximately, we can order the oxirane series according to decreasing D,

R,R-2,3-dimethyloxirane > S-methyloxirane > S-d_1-oxirane ≈ S,S-d_2-2,3-oxirane ≈ S-d_3-oxirane > S-methylthiirane,

or decreasing R,

S,S-d_2-2,3-oxirane > S-methyloxirane > R,R-2,3-dimethyloxirane > S-d_1-oxirane ≈ S-d_3-oxirane > S-methylthiirane,

or decreasing g_K,

TABLE II. Dipole (D/debye^2) and rotational (R/10^{-8} debye^2) strengths and the Kuhn parameter ($g_K = 4R/D$) in paramagnetic molecules, "randomly" selected, to illustrate typical and extreme values of g_K.

$N_{Ka,Kc}J$ (excited)	$N_{Ka,Kc}J$ (ground)	ν (GHz)	D	R	$g_K \times 10^6$
		S-d_1-oxirane radical			
$32_{1,32}$ 63/2	$31_{1,31}$ 61/2	906.702	0.343	−317	−37
$6_{0,6}$ 13/2	$5_{1,5}$ 11/2	178.149	0.401	198	20
$12_{12,1}$ 23/2	$12_{12,1}$ 25/2	1.585	0.003	2 979	43 921
		S,S-d_2-2,3-oxirane radical			
$34_{34,1}$ 69/2	$33_{33,1}$ 67/2	1782.952	0.935	−277	−12
$7_{0,7}$ 15/2	$6_{1,6}$ 13/2	190.615	0.758	271	14
$24_{14,10}$ 47/2	$23_{17,6}$ 47/2	0.0492	0.011	−2 641	−9 793
		S-d_3-oxirane radical			
$94_{0,94}$ 187/2	$93_{1,93}$ 185/2	2339.9235	0.405	132	13
$21_{1,20}$ 41/2	$20_{2,19}$ 39/2	545.1242	0.515	−172	−13
$5_{3,2}$ 11/2	$5_{2,3}$ 9/2	34.9812	0.007	−94	−507
		S-methyloxirane radical			
$75_{75,0}$ 151/2	$74_{74,1}$ 149/2	2893.4782	1.115	323	12
$36_{0,36}$ 73/2	$35_{1,35}$ 71/2	457.2821	0.993	−436	−18
$67_{36,32}$ 133/2	$68_{35,33}$ 135/2	0.6462	0.046	25 917	22 737
		S-methylthiirane radical			
$84_{84,1}$ 167/2	$83_{83,1}$ 165/2	2643.2293	0.419	183	17
$14_{13,2}$ 29/2	$13_{12,2}$ 27/2	411.4708	0.403	115	11
$12_{6,7}$ 23/2	$11_{7,4}$ 21/2	0.2512	0.021	1 074	2 053
		R,R-2,3-dimethyloxirane radical			
$87_{87,0}$ 175/2	$86_{86,0}$ 173/2	2165.9249	1.372	136	4
$40_{1,40}$ 81/2	$39_{0,39}$ 79/2	258.2400	1.302	374	12
$11_{5,7}$ 23/2	$12_{4,8}$ 25/2	0.1774	0.132	−6 333	−1 912

S-methyloxirane > *S*,*S*-d_2-2,3-oxirane > *S*-d_1-oxirane ≈ *S*-d_3-oxirane > *S*-methylthiirane > *R*,*R*-2,3-dimethyloxirane.

Absorption and RCD spectra simulated for *S*,*S*-d_2-2,3-oxirane, *S*-methyloxirane, and the two dialanine conformers at 2 K up to 50 GHz are plotted in Fig. 5. The effect of temperature is documented for *S*-methyloxirane in Fig. 6. The spectra were plotted with the Lorentzian bands, although at this scale the broadening is not visible. The four species dramatically differ in the density of the transitions, absorption, and RCD sign patterns. The density is mainly related to the rotational constant, which is largest for the dialanine conformers. Although for the two smaller molecules positive and negative RCD bands occur, within 1–100 GHz, the spectrum seems to be negatively biased for the first and positively biased for the second. The bias is more evident for dialanine, where RCD is positive and negative for the *cis*-I and *trans*-I conformer, respectively. This reflects a qualitative difference between RCD and electronic/vibrational CD spectroscopies. For ECD and VCD, zero-sum rules can be derived, and in a broader frequency region, the number of positive or negative bands is usually about equal.[35,51,52] As discussed previously,[17] these rules do not apply to RCD where the electronic and nuclear contributions are mixed differently. Nevertheless, even for both dialanine isomers, transitions with different signs exist, also apparent from the trends in Fig. 7.

B. Paramagnetic molecules

For paramagnetic molecules, some example transitions are listed in Table II and more of them in Table SVII. As expected, rotational strengths and Kuhn parameters are relatively large. The limits are given by the permanent dipole moments ($\mu \sim 10^0$ D, similar as for the diamagnetic molecules) and by the magnetic moment of the electron ($m \sim 10^{-2}$ D). A simple ratio $4m/\mu$ provides a g_K limit of $40\,000 \times 10^{-6}$. In Table II, we see that this value is achieved for the $12_{12,1}$ 25/2 → $12_{12,1}$ 23/2 transition in the *S*-d_1-oxirane radical. This transition, however, would be practically invisible in the spectra due to small populations of the involved states. For the other molecules, similar values appear, too, for transition frequencies below 1 GHz. Typical g_K factors in the radicals, however, are much smaller, only about ten-times larger than those seen in diamagnetic models.

For *S*,*S*-d_2-2,3-oxirane and *S*-methyloxirane radicals, the dependencies of *D*, *R*, and g_K on transition frequency ν and *J* are plotted in Fig. 8. As for the spinless case, the dipole strength quickly saturates with the transition frequency or *J*. Rotational strengths on average rise with *J*, but large values occur throughout the spectrum. In general, the lowest *J* spin-driven transitions provide large *R* and g_K, while for the highest ones, the rotational contribution to the magnetic moment becomes more apparent. A particular

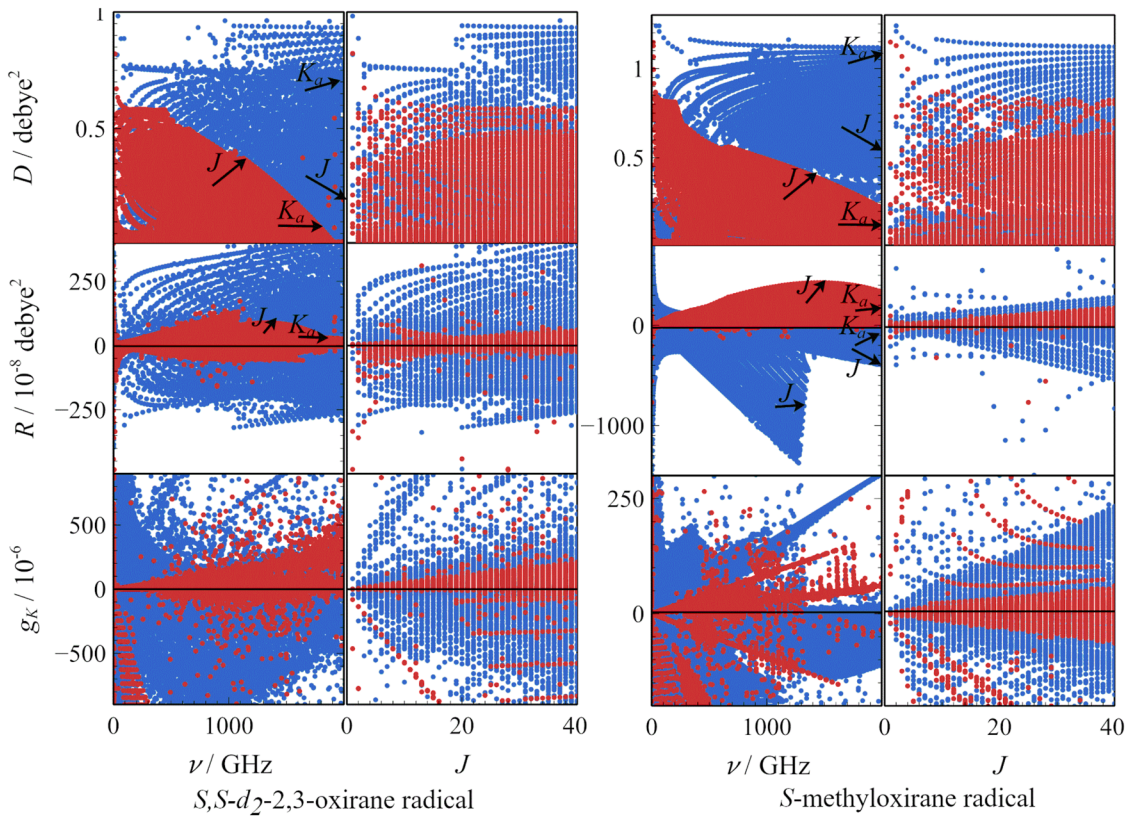

FIG. 8. *S*,*S*-d_2-2,3-oxirane and *S*-methyleneoxirane radicals, dipole and rotational strengths, and the g_K ratio dependent on the transition frequency ν and *J*; red for $\Delta J = 0$ and blue for $\Delta J = 1$.

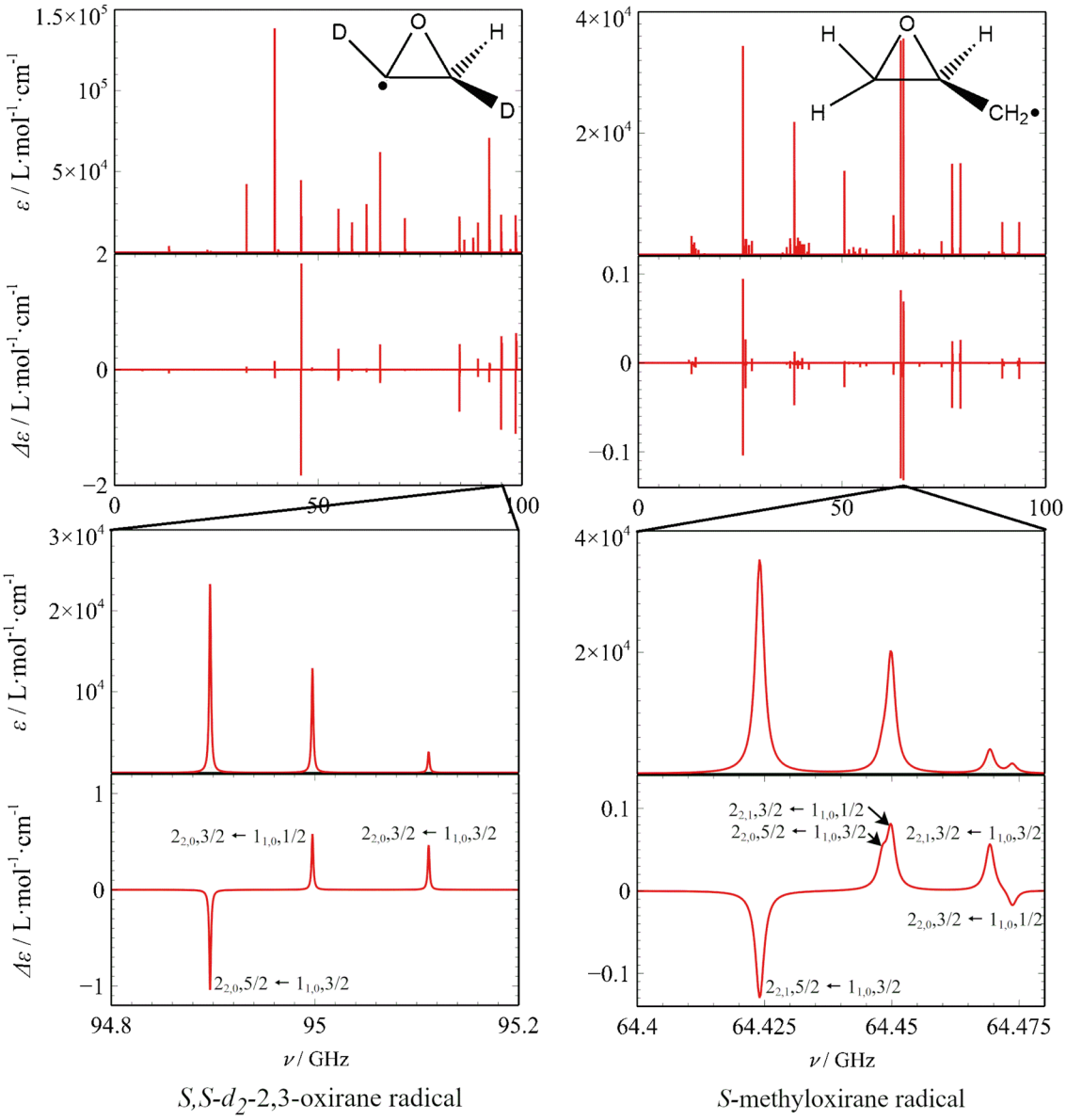

FIG. 9. Absorption and RCD spectra of *S,S*-d_2-2,3-oxirane and *S*-methyloxirane radicals; simulation in broader and narrower spectral regions.

spectral pattern, however, is very dependent on the kind of the radical.

RCD spectra of the paramagnetic molecules are not only more intense than for the closed shell systems but also more conservative; the number of positive and negative bands is about equal. This can be seen for *S,S*-d_2-2,3-oxirane and *S*-methyloxirane radicals in Fig. 9 (for other dia- and paramagnetic molecules, see Fig. S3). The same number of the positive and negative RCD bands reflects the fact that the magnetic part predominantly comes from the electronic (spin) contribution, at least at lower transition frequencies. Close-lying states where the rotational quantum number is the same but the spins are different also often produce "couplets," i.e., RCD bands close in frequency and absolute intensity, but of opposite signs. We observe this, for example, for the $0_{0,0}$ 1/2 → $1_{1,1}$ 1/2 and $0_{0,0}$ 1/2 → $1_{1,1}$ 3/2 transitions in the *S,S*-d_2-2,3-oxirane radical or for the $0_{0,0}$ 1/2 → $1_{1,0}$ 1/2 and $0_{0,0}$ 1/2 → $1_{1,0}$ 3/2 bands of the *S*-methyloxirane radical.

V. CONCLUSIONS

We have implemented the theory of rotational circular dichroism so that spectral intensities could also be computed for high-*J* transitions and paramagnetic radicals. The quadrupolar contribution to RCD has been included, but it did not contribute to the

spectrum for simulations conducted without external electric or magnetic fields. For diamagnetic molecules, simulations predict several interesting trends, such as the relatively high g_K = RCD/absorption ratios for high rotational quantum numbers. Overall, however, the ratios did not exceed 10^{-5} for $J < 100$. RCD spectra of the spinless systems are also often strongly nonconservative; especially for the dialanine conformers, predominantly one sign spectra are predicted. For the paramagnetic models, about 10–100 times g_K-factors were predicted, with $g_K \sim 4 \times 10^{-2}$ for a transition of the S-d_1-oxirane radical as an extreme value. RCD spectra of radicals were more conservative than for the diamagnetic molecules, and large intensities could be achieved already for low rotational quantum numbers. Unlike for electronic and vibrational CD, RCD spectra strongly depend on the temperature. We believe that the modeling may be useful as guidance for future RCD experiments.

SUPPLEMENTARY MATERIAL

See the supplementary material for the list of computational parameters, additional simulated data, the "RCD" program, and computational details.

ACKNOWLEDGMENTS

This work was supported by the Grant Agency of the Czech Republic (Grant No. 22-33060S).

AUTHOR DECLARATIONS

Conflict of Interest

The authors have no conflicts to disclose.

Author Contributions

Jiří Zdráhala: Investigation (equal); Methodology (equal); Software (lead); Validation (equal); Visualization (equal); Writing – review & editing (supporting). **Petr Bouř**: Conceptualization (lead); Funding acquisition (lead); Investigation (equal); Methodology (equal); Project administration (lead); Software (supporting); Visualization (equal); Writing – original draft (lead); Writing – review & editing (lead).

DATA AVAILABILITY

The data that support the findings of this study are available within the article and its supplementary material.

REFERENCES

[1]N. Berova, K. Nakanishi, and R. W. Woody, *Circular Dichroism Principles and Applications* (Wiley-VCH, New York, 2000).
[2]W. C. Johnson, Jr., in *Landolt Bornstein Numerical Data and Functional Relationships in Science and Technology*, edited by W. Saenger (Springer-Verlag, Berlin, 1990), p. 1.
[3]T. A. Keiderling, Chem. Rev. **120**, 3381 (2020).
[4]D. Kurouski, Anal. Chim. Acta **990**, 54 (2017).
[5]L. Nafie, *Vibrational Optical Activity: Principles and Applications* (Wiley, Chichester, 2011).
[6]J. Kessler *et al.*, Phys. Chem. Chem. Phys. **20**, 4926 (2018).
[7]S. A. Peebles *et al.*, J. Phys. Chem. A **113**, 3137 (2009).
[8]W. Gordy and R. L. Cook, *Microwave Molecular Spectra* (John Wiley & Sons, New York, 1984), pp. 523–528.
[9]T. J. Balle and W. H. Flygare, Rev. Sci. Instrum. **52**, 33 (1981).
[10]F. Xie *et al.*, Angew. Chem., Int. Ed. **59**, 22427 (2020).
[11]S. R. Domingos *et al.*, Chem. Sci. **11**, 10863 (2020).
[12]D. Patterson, M. Schnell, and J. M. Doyle, Nature **497**, 475 (2013).
[13]C. Lux *et al.*, Angew. Chem., Int. Ed. **51**, 5001 (2012).
[14]G. A. Garcia *et al.*, Nat. Commun. **4**, 2132 (2013).
[15]P. Herwig *et al.*, Science **342**, 1084 (2013).
[16]B. H. Pate *et al.*, in *Chiral Analysis*, edited by P. Polavarapu (Elsevier, 2018), p. 679.
[17]W. R. Salzman, J. Chem. Phys. **107**, 2175 (1997).
[18]W. R. Salzman, J. Chem. Phys. **94**, 5263 (1991).
[19]W. R. Salzman, Chem. Phys. **143**, 405 (1990).
[20]W. R. Salzman, Chem. Phys. **138**, 25 (1989).
[21]W. R. Salzman, J. Phys. Chem. **93**, 7351 (1989).
[22]W. R. Salzman, Chem. Phys. Lett. **141**, 71 (1987).
[23]W. R. Salzman, J. Chem. Phys. **67**, 291 (1977).
[24]W. R. Salzman, J. Mol. Spectrosc. **192**, 61 (1998).
[25]W. R. Salzman and P. L. Polavarapu, Chem. Phys. Lett. **179**, 1 (1991).
[26]P. L. Polavarapu, J. Chem. Phys. **86**, 1136 (1987).
[27]L. D. Barron and C. J. Johnston, J. Raman Spectrosc. **16**, 208 (1985).
[28]P. L. Polavarapu, Chem. Phys. Lett. **161**, 485 (1989).
[29]J. Šebestík and P. Bouř, J. Phys. Chem. Lett. **2**, 498 (2011).
[30]J. Šebestík and P. Bouř, Angew. Chem., Int. Ed. **53**, 9236 (2014).
[31]J. Šebestík *et al.*, Angew. Chem., Int. Ed. **55**, 3504 (2016).
[32]C. Meinert *et al.*, Nat. Commun. **13**, 502 (2022).
[33]D. Papoušek and M. R. Aliev, *Molecular Vibrational/Rotational Spectra* (Academia, Prague, 1982).
[34]P. R. Bunker and P. Jensen, *Molecular Symmetry and Spectroscopy* (NCR Research Press, Ottawa, 2006).
[35]L. D. Barron, *Molecular Light Scattering and Optical Activity* (Cambridge University Press, Cambridge, UK, 2004).
[36]J. R. Eshbach and M. W. P. Strandberg, Phys. Rev. **85**, 24 (1951).
[37]C. di Lauro and F. Lattanzi, in *Vibration-Rotational Spectroscopy and Molecular Dynamics*, edited by D. Papoušek (World Scientific, Singapore, 1997), p. 352.
[38]W. H. Flygare, Chem. Rev. **74**, 653 (1974).
[39]I. C. Bowater, J. M. Brown, and A. Carrington, Proc. R. Soc. London, Ser. A **333**, 265 (1973).
[40]R. N. Zare, *Angular Momentum* (John Wiley & Sons, New York, 1988).
[41]I. León *et al.*, Phys. Chem. Chem. Phys. **22**, 13867 (2020).
[42]B. A. McGuire *et al.*, Science **352**, 1449 (2016).
[43]Y. Hori *et al.*, Astrobiology **22**, 1330 (2022).
[44]B. Lankhaar, Astron. Astrophys. **666**, A126 (2022).
[45]M. J. Frisch *et al.*, Gaussian 16 (Revision C.01), (Gaussian, Inc., Wallingford, CT, 2016).
[46]S. Lehtola *et al.*, J. Chem. Theory Comput. **17**, 1457 (2021).
[47]J. Gauss, K. Ruud, and T. Helgaker, J. Chem. Phys. **105**, 2804 (1996).
[48]J. M. L. Martin, J. P. François, and R. Gijbels, J. Chem. Phys. **95**, 8374 (1991).
[49]H. M. Pickett *et al.*, J. Quant. Spectrosc. Radiat. Transfer **60**, 883 (1998).
[50]Z. Kisiel, in *Spectroscopy from Space*, edited by J. Demaison, K. Sarka, and E. A. Cohen (Springer, Dordrecht, The Netherlands, 2001), p. 91.
[51]A. Rupprecht, Mol. Phys. **63**, 955 (1988).
[52]P. L. Polavarapu, J. Chem. Phys. **84**, 542 (1986).